EVS24
Stavanger, Norway, May 13-16, 2009

Capacity Loss in Different Charge/Discharge Cycles of Lithium Ion Batteries

Peng Bai [1], Guangyu Tian, Quanshi Chen
State Key laboratory of Automotive Safety and Energy, Department of Automotive Engineering
Tsinghua University, Beijing, P. R. China
[1]Corresponding author, baif03@mails.tsinghua.edu.cn

Abstract

Lithium iron phosphate batteries, as the most promising candidate for EV/HEV power unit, are now under intensive R&D all over the world. Cycle performance experiments of a commercial $LiFePO_4$ conducted in Electric Vehicle Laboratory at Tsinghua University show that different charge/discharge cycles would lead to different capacity loss, this phenomenon is believed to be of considerable relevance with the mechanism of insertion/extraction in the cathode material. This paper, based on the shrinking core model, firstly explores the behaviour of the $LiFePO_4/FePO_4$ phase change in Lithium iron phosphate during charge/discharge schematically. Secondly, for improving the charge performance, a charge-discharge-charge profile is introduced to re-evaluate the shrinking core model for explain the capacity loss. Finally, based on the microscopic analysis, a schematic stochastic mosaic model is proposed, through which one can both learn how the battery really works and get valuable information for battery applications.

Keywords: lithium battery, modeling, battery charge, capacity

1 Introduction

Electric Vehicle (EV) and Hybrid Electric Vehicle (HEV) have been under intensive R&D as a would-be answer to the worldwide energy crisis and climate change. Batteries, as one of the most crucial technology for EV/HEV, with high power/energy density, rate capability and safety are considered to be the competitive candidates for future applications, among which $LiFePO_4$ batteries are the most promising one.

As everybody knows, poor conductivity hindered the development of $LiFePO_4$ becomes the most popular commercial battery today. Mechanism of insertion/extraction in Lithium iron phosphate is of clear relevance with the ion transport and electron conductivity during the battery reactions. For better understanding the performance in the cycles, especially under high C-rate conditions, capacity loss and its source have been discussed by many researchers ever since the $LiFePO_4$ was introduced to be a potential cathode material[1][2]. Padhi et al. [1] proposed the interface of phase transform reactions to explain the capacity loss under high current density. Andersson and Thomas [2] presented a radial model to analyze the capacity loss of $LiFePO_4$ cathode in the first cycle. Newman and co-workers [3] revealed the capacity loss in SEI formation. While the most scientists were focusing on the inherent capacity loss in battery cathodes, we have been conducting complete cell experiments toward EV applications. The term *capacity loss* in this paper is a profile-dependent property, and to some extent, it resembles the charge acceptance of batteries [4].

A lot of cycle performance experiments have been carried out by Electric Vehicle Division of State Key Laboratory of Automotive Safety and Energy in Tsinghua University. The results showed that different charge/discharge cycles lead to different capacity loss, which ignites the necessity of learning the basic mechanism of battery behaviour.

This paper, based on the shrinking core model, firstly explores the behaviour of the $LiFePO_4$/ $FePO_4$ phase change in Lithium iron phosphate during charge/discharge schematically. Secondly, for improving the charge performance, a charge-discharge-charge profile is introduced to re-evaluate the shrinking core model for explaining the capacity loss. What we present here is supposed to be coincide with the path-dependent phenomenon demonstrated by Venkat Srinivasan in [5], however, more detailed controls should be designed to explain the difference but beyond this study. Finally, based on the microscopic analysis, a schematic stochastic mosaic model is proposed, through which one can both learn how the battery really works and get valuable information for battery applications.

2 Experiment

Batteries used in this study were made by *Beijing Anhua United Power Co., Ltd* in China and composed of carbon coated $LiFePO_4$ cathode, LiPF6+EC electrolyte and LiC_6 anode. The stable capacity under C/3-rate gavanostatic condition is about 21Ah. Before we conducted the proposed experiments, the batteries were full activated and cycled under C/3-rate for several times. All the experiments were conducted with Arbin-EVTS Battery Cycler.

Here we proposed three constant-current (CC) charging profiles to demonstrate the profile-dependent capacity loss. As shown in Table 1, the first profile is a C/3-rate till upper limit charging, the second one consists of tow steps with the former under C/3-rate to the 60% SOC and the latter under C-rate till the upper limit; the last one consists of three steps with the sequence of 3C-rate→C-rate→C/3-rate, all of them were sustained till the upper limit of battery voltage.

Table1: Three CC profiles for charging

CC Profile	Step 1		Step 2		Step 3	
	I_C	Limit	I_C	Limit	I_C	Limit
1	C/3	3.65V	--	--	--	--
2	C/3	60%	C	3.65V	--	--
3	C/3	3.65V	C	3.65V	3C	3.65V

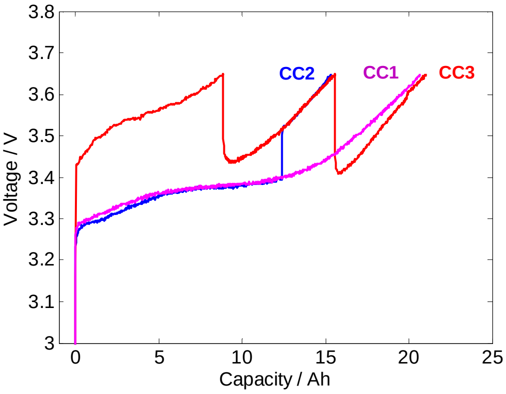

Fig. 1 Battery voltage under three CC profiles with respect to the charging capacity

Table2: Step values of charging capacity

Charge Capacity / Ah	C/3	C	3C
CC1	20.67	--	--
CC2	12.36	15.35	--
CC3	21.03	15.55	8.869

Each of the tests was repeated for 3 times, and the average results were plotted in Fig. 1. While C-rate and C/3-rate can reach about 15.5 Ah and about 20 Ah respectively, 3C-rate can only sustain to 8.869 Ah. From the results one can at least get two conclusions: (1) The higher the charging C-rate, the greater the charging capacity loss; (2) the battery can reserve more capacity through a relative smaller current even if the upper limit has been reached through a high C-rate. And thereby the charging capacity is dependent with the last sustained C-rate.

3 Model Development

It is interesting to find that the profile-dependent capacity loss is reversible by lowering the charging current. Study on how the battery really works will probably reveal this phenomenon.

3.1 Shrinking-core based analysis

Shrinking core model is prevailing in explaining and modeling battery behaviour [4][5][6][7]. According to the CC3 curve in Fig.1, there supposed to be three boundaries base on the core-shell mechanism. As shown in Fig.2, when the two phase reaction takes place, the phase boundary shrinks starting from the rim of the particle. Since the current is relevant with the total surface area of the boundary, a critical boundary will be formed under certain C-rate, the higher the current is, the greater the boundary surface area will be. So there

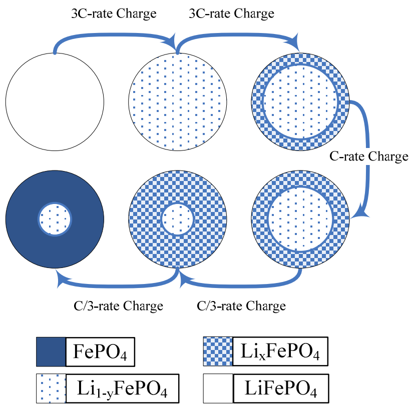

Fig. 2 Schematic presentation on capacity loss based on core-shell mechanism

will be an inert core of $Li_{1-y}FePO_4$ in the matrix as the interface shrinks to a critical surface area where the flux of lithium is no longer able to sustain the charge current, say C/3-rate [1].

In contrast, Fig.3 depicts a new procedure of charging. A discharge interval is applied into the constant charge process, which allows lithium ions insert into $LixFePO_4$ to form a $Li_{1-y}FePO_4$ ring. During the following charge process, the exterior interface of the ring will supply the critical flux to sustain the current, and the inert core will disperse onto the interior interface of the ring by diffusion, so that the current-supply interface, the exterior one, will not reach the critical surface area which means all $LiFePO_4$ will be consumed till the end of charge without any capacity loss. A new charging profile with a discharging interval was designed and tested.

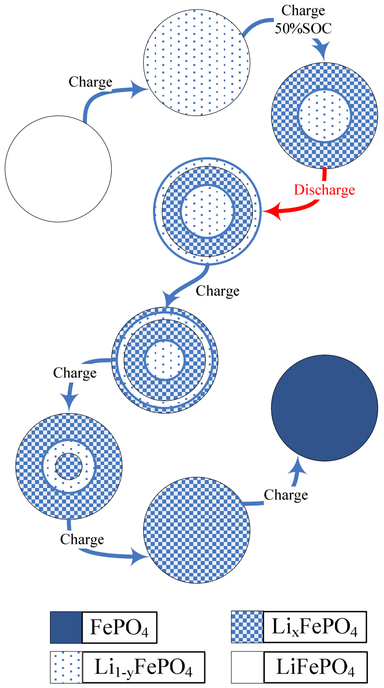

Fig. 3 Schematic presentation on phase transformation of Charge-Discharge-Charge

3.2 CDC profile

After several C/3-rate cycles, the charge-discharge-charge (CDC) experiments are carried out by the following steps listed in Table 4. The battery was firstly charged to 50% SOC under C/3-rate, and then discharged 10%, 20% and 30% SOC under C-rate, after which a 3C-rate current was applied to the battery till the upper limit.

The experimental results were plotted in Fig. 4, showing that the final capacities are different from we have expected. Although all the final capacities decrease from original 50% SOC, the CDC1 profile results in 9,283Ah, which is larger than the maximum 3C-rate capacity in Fig. 1, 8.869Ah.

It is clear the forgoing assumptions are invalidated by this experiment, and we need to explain this result through the core-shell mechanism.

Table1: Power levels for charging (230V)

CDC	Step 1		Step 2		Step 3	
	I_C	Limit	I_C	Limit	I_C	Limit
1	C/3	50%	-C	10%	3C	3.65V
2	C/3	50%	-C	20%	3C	3.65V
3	C/3	50%	-C	20%	3C	3.65V

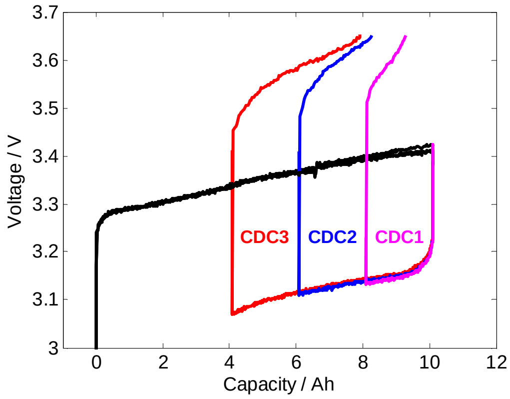

Fig. 4 Voltage-capacity relationship by CDC experiments

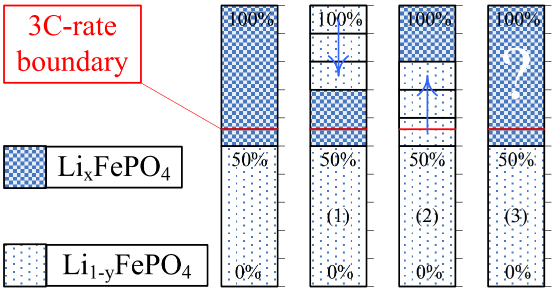

Fig. 5 Explanations on the CDC experiments

Table2: Step value of charging capacity

Charge Capacity / Ah	CDC1	CDC2	CDC3
Experimental	9.285	8.257	7.911
(1)	10.00	10.00	10.00
(2)	8.869	8.869	8.869
(3)	9.76	9.52	9.28

As we have demonstrated above, 3C-rate can only charge 8.869Ah into the battery, which means there exists an inherent critical boundary within which the 3C-rate cannot be sustained.

Assume that (1) the lithium ions insert back in step 2 starting from the outer rim of Li_xFePO_4 (100% line in Fig 5), then all the inserted lithium ions in step 2 are supposed to be drew out, because the boundary they formed is greater than the 3C-rate boundary, and the final capacity will at least be 10Ah if there isn't any lithium ions diffuse out off the $Li_{1-y}FePO_4$ core. On the other hand, assume that (2) the lithium ions insert back starting from the phase boundary of Li_xFePO_4/ $Li_{1-y}FePO_4$, then the inserted lithium ions on the top of red line are supposed to be extracted, and the final capacity after step 3 will definitely be 8,869Ah. However, as shown in Table 2, the expected results are highly different from the experimental ones. Next, assume that (3) the lithium ions insert into Li_xFePO_4 follow a roughly uniform distribution, which means that there will be 12% inserted lithium ions, in step 2, locating below the redline, then we get the expected results in the last row of Table 2, which are also different from the experiment.

This difficulty of explaining the capacity change in CDC experiments by using shrinking-core model makes us move toward the microscopic mechanism of lithium ion insertion/ extraction in $LiFePO_4$ cathode material.

3.3 Lithium insertion/extraction

Quantitative analysis on Li conductivity in a atomic-like channel formed by atoms in $LiFePO_4$ olivine structure, through which Li ions could migrate rapidly, has been investigated by D. Morgan and co-workers[8]. The authors have concluded that Li ions can rapidly migrating along *b* axis with little possibility for crossing between channels.

Gogi K. Singh et al [9] have proposed that random concentration fluctuations will generate concentration waves, which will travel along *a* axis (*x* axis), shown in Fig. 6. The blue shadow rectangle in the crystal is formed by the fast diffusion channels (thin blue lines) in *ab* plane. Li ions migrate (blue arrows) along *b* axis. The bold black lines in *ab* plane are the phase transformation wave fronts generated by concentration fluctuations, which can be treated as the infinitesimal slices of the phase boundary. And the red shadow triangles represent the stress fields, growing mainly along *c* axis.

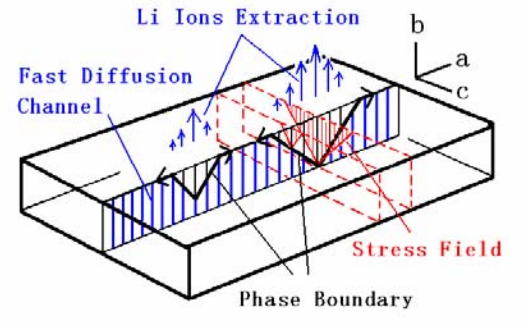

Fig 6. Relationship between phase boundary and stress field during Li extraction.

Guoying Chen et al [10] have proposed that，as Li ions leave the $LiFePO_4$ matrix along *b* axis, stress fields will be generated. Local bond stretching and bending in the phase boundary region may significantly enhance Li ion mobility.

Hence the transition zone can penetrate into the crystal as the stress field grows along the surface [10]. The authors have also proposed that the first nucleation sites will develop where the *ac* faces are well connected to the conducting matrix. If these are sufficient in number to supply enough lithium to maintain the charging current, growth of the new phase will be confined to those regions [10]. However, the increased applied potential will stimulate nucleation at less well-connected sites, providing an increased flow of Li ions from the particles. Rapid charging may also increase the stress at nucleation sites, and then expanding the disordered region through which the ions can move [10].

Combining the foregoing analysis, there exist two types of nucleation events: (1) triggered by random concentration fluctuations (2) triggered by stress fields, which are generated by previous nucleation. For the former type, Gogi K. Singh and co-workers have proposed the Poisson process to describe the general behaviour. As to the latter one, it is clear that the first nucleation is highly related with the following ones generated by its stress field, which may mainly grow along *c* axis and in other directions with minor possibility. However, here only the mainly growth is illustrated in Fig. 7. This figure can also illustrate the extraction in depth by

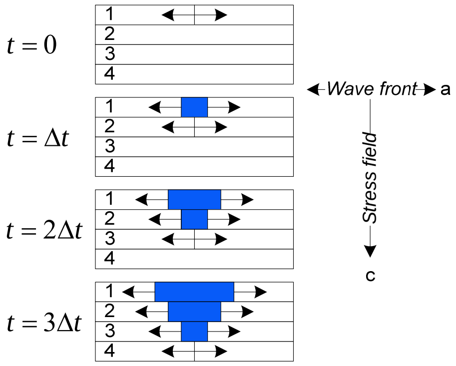

Figure 7. Stress field triggered nucleation.

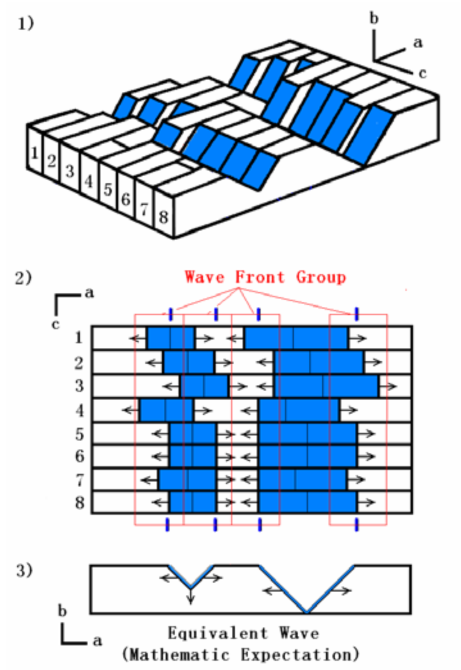

Fig 8. Schematic phase transformation travelling waves and the stress field

substituting the c axis with b axis. One can name this model as “cone”, which is analogous to the time cone [11].

Fig. 8 gives an illustration of a more general situation. There are 8 wave planes in the crystal and 4 wave fronts in each plane, travelling along *a* axis, shown in Fig. 8(1). According to the two types of nucleation, the adjacent wave fronts may travel within certain groups, such as the 8 rightmost wave fronts in Fig. 8(2). So that there must be a characteristic wave front to represent the behaviour of the grouped 8 wave fronts as a whole. Then the 8 infinitesimal slices of phase boundary would form a mathematical continuum boundary.

Furthermore, an over all equivalent wave plane for the crystal would be expected. Hence the microscopic mechanism of deintercalation is connected with the macroscopic behaviour through the mathematic expectation of a certain probability distribution of wave fronts. Based on all the analysis above, a preliminary schematic model for explaining the discharge process in one LiFePO4 particle is presented in Fig.9, named as stochastic mosaic model. The charging process in the two-phase region are expected to be different from the core-shell mechanism, rather than starting from the rim of the particle, nucleation firstly forms at some sites in the *ac* plane triggered by concentration fluctuations. Once the infinitesimal slices of phase boundary are developed, they will then travel along *a* axis while Li ions migrating perpendicularly out of the ac plane. According to the assumption by Gogi K. Singh et al, more and more nucleation events will be developed as a Poisson process. Driven by the voltage applied, waves will keep developing, travelling and impinging with each other and finally turn the $Li_{1-y}FePO_4$ into Li_xFePO_4. During this process, one cannot rule out the possibility of the formation of a continuous phase boundary, or at least an equivalent continuum boundary. It means that in some stage of the process, this model may equal to the shrinking core model [5], as they both have a continuum phase boundary. Actually they both represent the composition of Li-poor and Li-rich, the depth of delithiation.

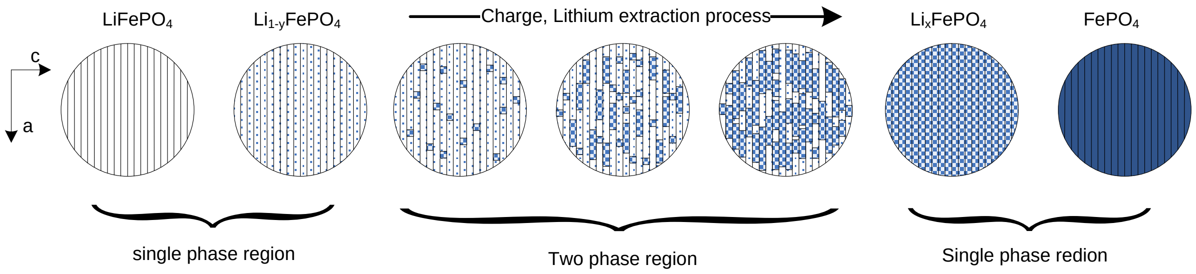

Figure 9. Stochastic mosaic model of LiFePO4 charging process

4 Future directions

Gogi K. Singh *et al* [9] have proposed the distribution of nucleation events during extraction is a Poisson process by assuming all electrode particles are at the same potential (driving force), which may only be true under low rate conditions or for thin electrodes. However, electrodes in many EV/HEV used batteries will frequently work under high rate conditions. Hence it is necessary to revise these assumptions for seeking another distribution of nucleation events. Its mathematic expectation is expected to be equivalent to the shrinking core model mathematically.

5 Conclusion

This paper firstly explored the behaviour of the $LiFePO_4/FePO_4$ phase change in charge process by using the shrinking core model schematically. And then a charge-discharge-charge profile was introduced to re-evaluate the shrinking core model for explain the capacity loss under different C-rate. Finally, based on the micro-scopic analysis, a schematic stochastic mosaic model was presented, through which one can learn how the battery really works. What we have been doing will provide more detail mechanism analysis on mathematic ground.

Acknowledgments

The authors thank Prof. Martin Z. Bazant for helpful comments on the schematic model of mosaic effect.

References

[1] A. K. Padhi, K. S. Nanjundaswamy, J. B. Goodenough, *Phospho-olivines as Positive-Electrode Materials for Rechargeable Lithium Batteries*, J. Electrochem. Soc., ISSN 0013-4651, 144, (1997) 1188-1194

[2] A. S. Andersson, J. O. Thomas, *The source of first-cycle capacity loss in LiFePO4*, Journal of Power Sources, ISSN 0378-7753, 97-98, (2001) 498-502

[3] J. Christensen, J. Newman, *Cyclable Lithium and Capacity Loss in Li-ion Cells*, J. Electrochem. Soc., ISSN 0013-4651, 152, (2005) A818-A829

[4] D. U. Sauer, E. Karden, B. Fricke et al, *Charging performance of automotive batteries — An underestimated factor influencing lifetime and reliable battery operation*, Journal of Power Sources, ISSN 0378-7753, 168, (2007) 22–30

[5] V. Srinivasan, J. Newman, *Existence of Path-Dependence in the $LiFePO_4$ Electrode*, J. Electrochem. Soc., ISSN 0013-4651, 9, (2006) A110-A114

[6] V. Srinivasan, J. Newman, *Discharge model for the lithium iron-phosphate electrode*, J. Electrochem. Soc., ISSN 0013-4651, 151, (2004) A1517-A1529

[7] Qi Zhang, Ralph E. White, *Moving Boundary Model for the Discharge of a $LiCoO_2$ Electrode*, J. Electrochem. Soc., ISSN 0013-4651, 154, (2007) A587-A596

[8] D. Morgan, A. Van der Ven, and G. Ceder, *Li Conductivity in $LiMPO_4$ (M = Mn, Fe, Co, Ni) Olivine Materials*, Electrochem. Solid- State Lett., ISSN 1099-0062, 7, (2004) A30-A32

[9] Gogi K. Singh, Gerbrand Ceder, Martin Z. Bazant, *Intercalation dynamics in rechargeable battery materials: General theory and phase transformation waves in $LiFePO_4$*, Electrochim. Act., ISSN 0013-4686, 53, (2008) 7599-7613

[10] Guoying Chen, Xiangyun Song, and Thomas J. Richardson, *Electron Microscopy Study of the $LiFePO_4$ to $FePO_4$ Phase Transition*, Electrochem. Solid-State Lett., ISSN 1099-0062, 9, (2006) A295-A298

[11] Robert W. Balluffi, Samuel M. Allen, W. Craig Carter, *Kinetics of Materials*, ISBN 13 978-0-471-24689-3, chapter 21, John Wiley & Sons., Hoboken, NJ, 2005.

Authors

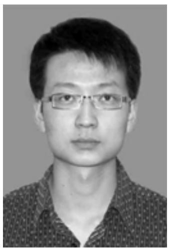

Peng Bai, received the B.E degree from Tsinghua University, Beijing, China, in 2007, and is currently pursuing the Ph.D. degree at Tsinghua University. His recent interest is focused on electrochemical analysis and mathematical modeling of $LiFePO_4$ batteries toward EV/HEV applications.

Guangyu Tian, received the B.E, M.E and Ph.D. degrees from Tsinghua University, Beijing, China, in 1986, 1991 and 1995, respectively, and then joined the faculty in Dept. Automotive Engineering at Tsinghua University. Research interests include application and control study of advanced power sources and systems, modeling and simulation of EV/HEV systems.

Quanshi Chen, received the B. E degree in automotive engineering from Tsinghua University, Beijing, China, in 1970. He then joined the faculty in Dept. Automotive Engineering at Tsinghua University. He is the Director of State Key laboratory of Automotive safety and Energy, and has been leading the EV/HEV R&D for decades in China. Research interests include application and control study of advanced power sources and systems, modeling and simulation of EV/HEV systems.